

11-2010

**REGULATION OF INTEGRIN  $\alpha$ IIb $\beta$ 3 LIGAND BINDING AND  
SIGNALING BY THE METAL ION BINDING SITES IN THE  $\beta$  I  
DOMAIN**

Joel Raborn

Follow this and additional works at: [https://digitalcommons.lsu.edu/honors\\_etd](https://digitalcommons.lsu.edu/honors_etd)

 Part of the [Biology Commons](#)

---

**REGULATION OF INTEGRIN  $\alpha$ IIb $\beta$ 3 LIGAND BINDING AND SIGNALING BY THE  
METAL ION BINDING SITES IN THE  $\beta$  I DOMAIN**

by

Joel Raborn

Undergraduate honors thesis under the direction of

Dr. Bing-Hao Luo

Department of Biological Sciences

Submitted to the LSU Honors College in partial fulfillment of  
the Upper Division Honors Program.

November 2010

Louisiana State University  
& Agricultural and Mechanical College  
Baton Rouge, Louisiana

## ABSTRACT

The ability of  $\alpha\text{IIb}\beta\text{3}$  to bind ligands and undergo outside-in signaling is regulated by three divalent cation binding sites in the  $\beta$  I domain. Specifically, the metal ion-dependent adhesion site (MIDAS) is the site of ligand binding because the MIDAS  $\text{Mg}^{2+}$  coordinates with the ligand during binding, and the synergistic metal binding site (SyMBS) coordinates  $\text{Ca}^{2+}$  while stabilizing the MIDAS for binding. Both are thought to be required for ligand binding due to their synergy between  $\text{Ca}^{2+}$  and  $\text{Mg}^{2+}$ . The adjacent to MIDAS (ADMIDAS) is an important ligand binding regulatory site that stabilizes the MIDAS and also acts as a critical link between the  $\beta$  I and hybrid domains for signaling. Previous mutagenesis studies with the ADMIDAS have provided conflicting results for ligand binding and adhesion in different integrins. We have mutated the  $\beta\text{3}$  SyMBS and ADMIDAS. The SyMBS mutants abolished ligand binding and outside-in signaling, but when a glycosylation mutation in the  $\alpha\text{IIb}$  Calf 2 domain was introduced that activated the integrin to the high affinity state, the ligand binding affinity and signaling were restored. Thus, the SyMBS is important but not absolutely required for integrin bidirectional signaling. The ADMIDAS mutants showed reduced ligand binding affinity and abolished outside-in signaling, and the same activating glycosylation mutation could fully restore integrin signaling of the ADMIDAS mutant. We propose that the ADMIDAS ion stabilizes the low affinity state when the integrin headpiece is in the closed conformation, whereas it stabilizes the high affinity state when the headpiece is in the open conformation with the swung-out hybrid domain.

## INTRODUCTION

Integrins are cell adhesion receptors involved in multiple biological processes including development, cancer, hemostasis, and immune response through cell-cell, cell-extracellular matrix (ECM), and cell-pathogen interactions (1-2). Composed of a large extracellular domain, a short transmembrane domain, and a short cytoplasmic domain connected to the cytoskeleton, integrins transmit signals via inside-out and outside-in signaling. Integrins are usually in the low affinity state with the extracellular domain in the bent conformation in normal physiological conditions. When the cell is stimulated by external agents, specific intracellular molecules interact with the integrin cytoplasmic domain, resulting in conformational change leading to integrin extension into the high affinity state (3-7). Furthermore, ligand binding can induce outside-in signaling and activate many intracellular signaling pathways (8-11).

It has been known that integrin affinity for ligands is regulated by metal ions (12-16). Some divalent cations such as  $Mn^{2+}$  can activate integrins for ligands, whereas  $Ca^{2+}$  typically favors the inactive state. Crystallographic studies of the  $\alpha V\beta 3$ ,  $\alpha IIb\beta 3$ , and  $\alpha M\beta 2$  in the unliganded closed conformations (17-19) and of the  $\alpha IIb\beta 3$  in the liganded open conformation (3) have provided the structural basis for the cation dependence for ligand binding. Within the extracellular domain, the  $\alpha I$  domain, which was found in half of the integrins, is responsible for ligand binding. In integrins that lack the  $\alpha I$  domain such as the  $\beta 3$  integrins, the  $\beta I$  domain is the main binding site for ligands (3-5,7,18,20-21). The  $\beta I$  domain contains three metal ion coordinating sites that are important for ligand binding and signaling. First, the metal ion dependent adhesion site (MIDAS) binds to a specific anionic sequence on ligands and coordinates  $Mg^{2+}$  under normal physiological conditions (14-15,20-22). The MIDAS contains a conservative motif DXSXS (Fig. 1) and is at the center of the three metal ion cluster. This

DXSXS motif is essential for coordinating the metal ion, which is critical for ligand binding (23-24). Structural studies have revealed the carboxyl group of Asp in the RGD sequence of the ligand coordinates with the MIDAS  $Mg^{2+}$  of the  $\beta 3$  subunit during ligand binding, indicating that the MIDAS is essential for ligand binding (3-4). This was supported by mutagenesis studies in which mutations in the MIDAS site completely abolished ligand binding (25-27). Next, the synergistic metal binding site (SyMBS, previously known as ligand-associated metal binding site or LIMBS) coordinates  $Ca^{2+}$  and allosterically activates integrins for ligand binding by stabilizing the MIDAS site (19,28). The SyMBS in low  $Ca^{2+}$  concentration will synergize with low concentration of MIDAS  $Mg^{2+}$  to facilitate the ligand binding (19). The mutations in the SyMBS in various integrin families have reduced or abolished ligand binding, while this abnormal ligand binding can be restored by the activating mutations of the  $\alpha$  I domain or a glycosylation mutation that stabilized the integrin headpiece in the open conformation (14-15,25-26,29-31). Finally, the adjacent to MIDAS (ADMIDAS) was proposed to allosterically inhibit ligand binding when coordinated with  $Ca^{2+}$  (14,22,25-26). The linkage between the  $\beta$  I domain ADMIDAS and the hybrid domain essential for integrin signaling creates a unique biological role for the ADMIDAS (25,32). This site was thought to orchestrate between ligand-binding inhibition and propagation of the signal to the inside of the cell (3-4,17,25-26). Mutations in the ADMIDAS have abolished integrin outside-in signaling, but either increased or decreased ligand binding affinity was observed in different integrins (14-15,22,25-26,33). In studies with  $\alpha L\beta 2$  and  $\alpha 4\beta 7$ , mutations in the ADMIDAS increase ligand binding and firm adhesion compared to the wild type (WT) (14-15,25). By contrast, the ADMIDAS mutations in  $\alpha 5\beta 1$  and  $\alpha 2\beta 1$  decreased ligand binding (22,26). It remains elusive how to reconcile these conflicting observations.

In this paper, we introduced specific mutations into the SyMBS and ADMIDAS to study the role of these metal ion complexes in  $\alpha$ IIb $\beta$ 3 ligand binding and outside-in signaling. Our results showed that the SyMBS mutants abolished ligand binding and outside-in signaling, but when an activating glycosylation mutation was introduced into the lower legs to disrupt the  $\alpha\beta$  association, the ligand binding and signaling were restored. The ADMIDAS mutants showed reduced ligand binding affinity and abolished outside-in signaling. The activating glycosylation mutation could fully restore the functions of the ADMIDAS mutant. The study provides insight into the role of these two metal ion binding sites in integrin ligand binding and signaling.

## **EXPERIMENTAL PROCEDURES**

*Plasmid Construction and Expression*—Plasmids with sequences for full-length human  $\alpha$ IIb and  $\beta$ 3 were subcloned into pEF/V5-HisA and pcDNA3.1/Myc-His (+), respectively (34). The  $\alpha$ IIb mutants F755T and the  $\beta$ 3 mutants D126A, D127A, and D217A were made using site-directed mutagenesis with the QuikChange kit (Stratagene, La Jolla, CA). Constructs were transfected into HEK293T cells (American Type Culture Collection, Manassas, VA) using a FuGENE transfection kit (Roche Applied Science, Indianapolis, IN) according to the manufacturer's instructions. The expression levels of  $\alpha$ IIb and  $\beta$ 3 were detected by flow cytometry staining with the following monoclonal antibodies: AP3 (nonfunctional anti- $\beta$ 3 mAb, American Type Culture Collection), 7E3 (anti- $\beta$ 3 mAb), 10E5 (anti- $\alpha$ IIb mAb, kindly provided by B. S. Coller, Rockefeller University, New York, NY), and LM609 (anti- $\alpha$ V mAb).

*Two-Color Ligand Binding Assay on HEK293T Transfectants*—Soluble binding of ligand mimetic IgM PAC-1 (BD Biosciences, San Jose, CA) and Alexa Fluor 488-labeled human fibrinogen (Enzyme Research Laboratories, South Bend, IN) was determined as previously described (35). Briefly, transfected cells suspended in 20 mM HEPES-buffered saline, pH 7.4

(HBS) supplemented with 5.5 mM glucose and 1% bovine serum albumin (BSA) were incubated on ice for 30 min with 10 µg/mL PAC-1 or 10 µg/mL Alexa Fluor 488-conjugated human fibrinogen in the presence of either 5 mM EDTA, 5 mM Ca<sup>2+</sup>, or 1 mM Mn<sup>2+</sup>. For PAC-1 binding, cells were washed and stained with FITC-conjugated anti-mouse IgM on ice for another 30 min before being subjected to flow cytometry. Cells were also stained in parallel with Cy3-conjugated anti-β3 mAb AP3. Binding activity is presented as the percentage of the mean fluorescence intensity (MFI) of PAC-1 or fibrinogen staining after background subtraction of the staining in the presence of EDTA, relative to the MFI of the AP3 staining.

*Ligand-Induced Binding Site (LIBS) Epitope Expression*—LIBS epitope expression was measured as previously described (35). Briefly, transfected cells suspended in HBS supplemented with 5.5 mM glucose and 1% BSA were incubated for 15 min at room temperature (RT) with or without 50 µM GRGDSP peptide in the presence of 5 mM Ca<sup>2+</sup> or 5 mM Mn<sup>2+</sup>. Then, cells were stained with 10 µg/ml anti-LIBS1 antibody or 10 µg/ml anti-LIBS6 antibody and incubated on ice for 30 min. After incubation on ice for 30 min, cells were washed and stained with FITC-labeled anti-mouse IgG on ice for 30 min. The stained cells were subjected to flow cytometry, and LIBS1 and LIBS6 epitope expression was expressed as the percentage of MFI of anti-LIBS antibody relative to MFI of the conformation-independent anti-β3 mAb AP3.

*Cell Adhesion Assays*—Cell adhesion on immobilized human fibrinogen was assessed by the measurement of cellular lactate dehydrogenase (LDH) activity as previously described (11). Briefly, cells suspended in HBS supplemented with 5.5 mM glucose and 1% BSA and 1 mM Ca<sup>2+</sup> were added into flat bottom 12-well plates (1 × 10<sup>5</sup> cells/well) precoated with 20 µg/ml fibrinogen and blocked with 1% BSA. After incubation at 37 °C for 30 min, wells were washed three times with HBS supplemented as indicated above. Remaining adherent cells were lysed

with 1% Triton X-100, and LDH activity was assayed using the Cytotoxicity Detection Kit (Roche Applied Science) according to the manufacturer's instructions. Cell adhesion was expressed as a percentage of bound cells relative to total input cells.

*Cell Spreading and Microscopy*— Glass bottom 6-well plates (MatTek Corporation, Ashland, MA) were coated with 20  $\mu\text{g}/\text{mL}$  human fibrinogen in phosphate-buffered saline at pH 7.4 (PBS) overnight at 4  $^{\circ}\text{C}$ , and then blocked with 1% BSA at RT for 1 h. The transiently transfected HEK293T cells were detached with trypsin/EDTA, washed three times with DMEM, and seeded on fibrinogen-coated plates. After incubation at 37  $^{\circ}\text{C}$  for 1 h, cells were washed three times with PBS and fixed with 3.7% formaldehyde in PBS at RT for 10 minutes for microscopy.

Differential interference contrast (DIC) imaging was conducted on a Leica TCS SP2 spectral confocal system coupled to a DM IRE2 inverted microscope with a 63X oil objective. For the quantification of cell spreading area, outlines of 100 randomly selected adherent cells were generated, and the number of pixels contained within each of these regions was measured using ImageJ software (Bethesda, Maryland).

## RESULTS

*Design and Expression of Mutant  $\alpha\text{IIb}\beta 3$  Integrins.* Based on the crystal structure of the  $\alpha\text{IIb}\beta 3$  integrin, several point mutations in the SyMBS and ADMIDAS sites in the  $\beta 3$   $\beta$  I domain were created to change Asp to Ala. By replacing the Asp with the non-polar amino acid, the SyMBS and ADMIDAS were expected to be disrupted, accordingly their functions could be eliminated. Also, a glycosylation point mutation was created in the  $\alpha\text{IIb}$  Calf-2 domain,  $\alpha\text{IIb\_F755T}$  (denoted F755T), which results in N-glycosylation of  $\alpha\text{IIb}$  N753 in the interface of Calf-2 domain and the  $\beta 3$  EGF-4 domains and thus disrupts the two leg association. The mutant has been shown to cause full activation of the  $\alpha\text{IIb}\beta 3$  integrin (36). To determine the expression



of integrins on the cell surface, the WT and mutant  $\alpha$ IIB $\beta$ 3 were co-transfected into HEK293T cells and subjected to immunostaining flow cytometry. To exclude the possible contribution of endogenous  $\alpha$ V or  $\beta$ 3 in HEK293T cell lines, anti- $\alpha$ V antibody LM609 was used and we did not detect any endogenous  $\alpha$ V or  $\beta$ 3 expression. When  $\alpha$ V and  $\beta$ 3 subunits were co-transfected into this cell line, the  $\alpha$ V expression can be detected using LM609, suggesting that the antibody is functional (data not shown). Furthermore, when the WT and mutant  $\alpha$ IIB $\beta$ 3 integrins were co-transfected, LM609 did not bind to the cells (Fig. 2), confirming that no endogenous  $\alpha$ V was expressed that could potentially complicate our experiments. Two anti- $\beta$ 3 antibodies AP3 and 7E3, which recognize the hybrid and the  $\beta$ 3 I domains, respectively, and one anti- $\alpha$ IIB antibody 10E5, which recognizes the  $\beta$ -propeller domain, were used to monitor cell surface expression of the transfected  $\alpha$ IIB $\beta$ 3 integrins. Wild-type and mutant integrins bound to the three antibodies with similar level (Fig. 2), suggesting that all mutations have little effect on protein expression, and they adopted a native structure on the cell surface. Therefore, none of the mutants had any effect on integrin global conformation.

*Regulation of PAC-1 and Fibrinogen binding by the SyMBS and ADMIDAS sites.* Two-color flow cytometry was used to determine the fibrinogen and ligand mimetic PAC-1 binding of the WT and mutants. In the presence of  $\text{Ca}^{2+}$ , WT  $\alpha$ IIB $\beta$ 3 bound very little ligand-mimetic PAC-1 antibody or fibrinogen. This is consistent with a low-affinity state under the physiological condition. In the presence of  $\text{Mn}^{2+}$ , WT  $\alpha$ IIB $\beta$ 3 bound PAC-1 and fibrinogen with higher affinity, suggesting that  $\text{Mn}^{2+}$  could slightly activate integrin  $\alpha$ IIB $\beta$ 3 for ligand binding, even though the activation effect is lower than the glycosylated mutant F755N. This F755T mutant caused a three to four fold increase in ligand binding compared to the WT  $\alpha$ IIB $\beta$ 3, which

appeared to have maximum ligand binding in  $\text{Ca}^{2+}$ , and  $\text{Mn}^{2+}$  could not further enhance its binding, consistent with our previous observation (Fig. 3) (36).

By contrast, the D217A SyMBS mutant severely inhibited ligand binding, and even  $\text{Mn}^{2+}$  could not activate the mutant for PAC-1 or fibrinogen binding (Fig. 3). The data suggest that the SyMBS site is important for ligand binding and integrin is inactivated when the SyMBS site is abolished. However, this mutation, when combined with the F755T glycosylation mutation, appears to recover the ability of ligand binding. The F755T/D217A double mutant showed higher binding to PAC-1 in  $\text{Ca}^{2+}$  compared to the WT, and the presence of  $\text{Mn}^{2+}$  could not further increase its binding. In soluble fibrinogen binding, the F755T/D217A double mutant exhibited much higher binding compared to the WT both in  $\text{Ca}^{2+}$  and  $\text{Mn}^{2+}$ . Therefore, mutation that disrupts the association of the two integrin legs could restore the SyMBS mutant, suggesting that SyMBS is important, but not absolutely required for integrin ligand binding.

Two ADMIDAS mutations D126A and D127A showed almost no binding to soluble PAC-1 or fibrinogen in  $\text{Ca}^{2+}$ , similar to the WT, suggesting that the mutants do not enhance binding affinity. The presence of  $\text{Mn}^{2+}$  could slightly increase the mutants for ligand binding, indicating that integrins with ADMIDAS abolishment are still sensitive to  $\text{Mn}^{2+}$  activation. However, both mutants exhibited reduced ligand binding affinity compared to the WT in  $\text{Mn}^{2+}$ . These mutants bound soluble PAC-1 with significantly lower binding affinity compared to the WT; whereas their binding to fibrinogen was only slightly reduced. Interestingly, the glycosylated double mutant F755T/D127A showed almost maximal affinity to both PAC-1 and fibrinogen, in either  $\text{Ca}^{2+}$  or  $\text{Mn}^{2+}$  conditions (Fig. 3). Our results indicate that the ADMIDAS is important for regulating integrin ligand binding affinity, but its role is more complicated.

*Conformational changes induced by SyMBS and ADMIDAS mutants.* Priming and ligand binding induce  $\alpha$ IIB $\beta$ 3 conformational changes that expose the LIBS epitopes. LIBS epitopes are at the interfaces between the headpiece and tailpiece and between the  $\alpha$  and  $\beta$  legs so that they are buried in the bent conformation but exposed in the extended conformation (34,37). To investigate the conformational state of the  $\alpha$ IIB $\beta$ 3 mutants, binding of anti- $\beta$ 3 LIBS mAb LIBS1 and LIBS6 (38) was measured in various conditions of  $\text{Ca}^{2+}$ ,  $\text{Ca}^{2+}/\text{RGD}$ ,  $\text{Mn}^{2+}$ , and  $\text{Mn}^{2+}/\text{RGD}$ . The LIBS1 and LIBS6 bound poorly to wild-type  $\alpha$ IIB $\beta$ 3 in the presence of  $\text{Ca}^{2+}$  alone. The presence of  $\text{Mn}^{2+}$  or the ligand mimetic peptide GRGDSP could increase the antibody binding, whereas the binding significantly increased when both  $\text{Mn}^{2+}$  and RGD were added (Fig. 4), suggesting that the RGD peptide with  $\text{Mn}^{2+}$  stabilizes integrins in the more open conformation. The glycosylated mutant F755T bound LIBS1 and LIBS6 antibodies even in  $\text{Ca}^{2+}$ , comparable to the WT in the presence of  $\text{Mn}^{2+}/\text{RGD}$  (Fig. 4). The data confirm that the separation of the two legs stabilizes integrins in a more open, high affinity conformation, consistent with our previous observation (36).

The SyMBS mutant D217A exhibited lower binding to LIBS1 and LIBS6 under  $\text{Ca}^{2+}$  than the WT, suggesting that this mutant is likely in the more bent conformation. The presence of  $\text{Ca}^{2+}/\text{RGD}$ ,  $\text{Mn}^{2+}$ , or  $\text{Mn}^{2+}/\text{RGD}$  had almost no effect on LIBS1 and LIBS6 binding. Therefore, the SyMBS mutation not only inhibited ligand binding but also caused the integrin to remain in the bent conformation, regardless of whether  $\text{Mn}^{2+}$  or RGD was added. The glycosylated double mutant F755T/D217A showed significantly higher binding to LIBS1 and LIBS6 compared to the WT and the D217A mutant (Fig. 4), suggesting that separation of the two legs shifts the equilibrium of integrin conformations towards a more open conformation even though the SyMBS was abolished. This global conformational change induced by the glycosylation may

explain the higher binding affinity of this double mutant to soluble PAC-1 and fibrinogen as shown above.

The ADMIDAS mutants D126A and D127A showed similar LIBS1 and LIBS6 binding as the WT in the presence of  $\text{Ca}^{2+}$ . Whereas these two mutants bound to LIBS1 and LIBS6 with significantly lower levels compared to the WT in the presence of  $\text{Mn}^{2+}$  and  $\text{Mn}^{2+}/\text{RGD}$ . These data suggest that the ADMIDAS mutants remain in the bent conformation even in the  $\text{Mn}^{2+}$  and/or RGD conditions. The glycosylated double mutant F755T/D127A showed higher binding to LIBS1 and LIBS6 than the WT in  $\text{Ca}^{2+}$ , confirming that the F755T/D127A mutant is in the more open conformation (Fig. 4).

*Effects of SyMBS and ADMIDAS mutants on adhesion and spreading.* Cell adhesion on the immobilized fibrinogen was assessed using cytotoxicity detection kit of LDH, the adhesion percentage was calculated by ratio of adherent cells to the total input cells. About 50% of the HEK293T cells transiently transfected with the WT adhered to the immobilized fibrinogen, while the glycosylated mutant F755N showed slightly increased adhesion (Fig. 5A). In contrast, the SyMBS mutant D217A almost abolished the adhesion. The double mutant F755N/D217A could adhere to the immobilized fibrinogen even though with lower ratio compared to the WT (Fig. 5A), suggesting that the separation of the two legs could partially restore the cell adhesion ability of the SyMBS mutant. The adhesion of ADMIDAS mutants D126A and D127A was about 60% of the WT, which correlated to their decreased ligand-binding ability and increased tendency toward the bent conformation compared to the WT. The double mutant F755N/D127A increased the adhesion to a similar level to the WT (Fig. 5A).

To test if mutations of metal ion sites could affect integrin outside-in signaling, HEK293T transient transfectants were coated on immobilized fibrinogen at 37 °C for 1 h,

followed by fixation and microscopic analysis to determine cell spreading of the mutants. Cells transfected with the WT showed normal cell adhesion and spreading (Fig. 5B). No spreading data were obtained for the SyMBS mutation, since there was no adhesion. The glycosylated double mutant F755T/D217A partially restored the cell adhesion, and those cells that adhered to immobilized fibrinogen showed significant spreading (Fig. 5C). The cell area was quantified, and the data showed that this double mutant had larger cell size compared to the two ADMIDAS mutants, but was slightly smaller than the WT (Fig. 5B).

Two ADMIDAS mutants D126A and D127A exhibited defective spreading on fibrinogen (Fig. 5C), and even though some cells could adhere to the immobilized fibrinogen, they remained round and did not change size. Quantification of the cell area showed that these two mutants had a significant decrease in adherent cell size comparing to that of the WT (Fig. 5B). The glycosylated double mutant F755T/D127A could adhere and spread on immobilized fibrinogen almost as well as the WT. The data suggest that separation of two legs could restore cell spreading capability of the ADMIDAS mutant. Thus, the glycosylated mutation that disrupts the two leg association was able to reestablish the cell adhesion and spreading in the SyMBS and ADMIDAS mutations.

## **DISCUSSION**

We made several  $\beta 3$  integrin SyMBS and ADMIDAS mutants and studied their effect on  $\alpha$ IIB $\beta$ 3 ligand binding and signaling. The SyMBS mutation almost completely abolished ligand binding, conformational change into the active state, and integrin outside-in signaling; whereas the glycosylated mutant that disrupts integrin lower leg association could restore its function. The ADMIDAS mutant decreased integrin ligand binding and abolished outside-in signaling, but this mutant was sensitive to  $Mn^{2+}$  activation. Therefore, the role of the ADMIDAS is more

complicated, and the glycosylated mutant could fully restore the function of the ADMIDAS mutant.

It has been shown that the side chain carboxyl of  $\beta 3$  subunit Glu<sup>220</sup> coordinates the SyMBS Ca<sup>2+</sup> and MIDAS Mg<sup>2+</sup> at the same time in both the unliganded low-affinity state and the liganded high-affinity state (Fig. 1B and 1C) (3,19). Therefore, the presence of the SyMBS Ca<sup>2+</sup> may favor the specific orientation of this side chain carboxyl to stabilize the MIDAS ion occupancy. Consequently, SyMBS acts as a stimulatory site of Ca<sup>2+</sup> as shown in  $\alpha 2\beta 1$  (26). Our study confirmed that the metal ion in the SyMBS is critical for integrin  $\alpha IIb\beta 3$  bidirectional signaling. Similar results have been reported that the SyMBS mutants abolish ligand binding and conformational change into the extended state in the  $\alpha 2\beta 1$  (26),  $\alpha 5\beta 1$  (22),  $\alpha 4\beta 7$  (14-15), and  $\alpha L\beta 2$  (25) integrins; and the effects of SyMBS mutations in shear flow have resulted in rolling rather than firm adhesion (14-15,25). In  $\alpha IIb\beta 3$ ,  $\beta 3$  SyMBS mutations were also reported to abolish ligand binding (29,39-41). Together, these studies demonstrate the similar function of the SyMBS among different  $\beta$  subunit I domains and between integrins with and without the  $\alpha$  I domain. Our study here showed that glycosylated mutant that disrupts integrin lower leg association could restore the SyMBS mutant for ligand binding and signaling. We have shown that the glycosylation caused global conformational change resulting in increased ligand binding affinity (36). It is possible that separation of the two legs leads to integrin extension with open headpiece conformation, causing metal ion occupied in the MIDAS capable of binding ligand and signaling. Similar results were obtained in  $\alpha 4\beta 7$  integrin where glycan wedge was introduced at the interface of the  $\beta$  I and hybrid domains to stabilize the integrin in the open headpiece conformation (15). This glycan wedge mutant could restore the SyMBS mutants for ligand binding, conformational change, and cell adhesion. Therefore, it seems that the SyMBS is

important, but not absolutely required, for integrin signaling, and integrins in the extended conformation with open headpiece could counteract the SyMBS mutant.

It was proposed that the ADMIDAS is an allosteric inhibitor of ligand binding when bound to  $\text{Ca}^{2+}$  and functions as a critical connection between the  $\beta$  I domain with hybrid domain in outside-in signaling (14-15,22,26). However, ADMIDAS mutants produced conflicting results by either increasing or decreasing ligand binding in different integrins (14-15,22,26,33). Our study showed that the  $\beta 3$  ADMIDAS mutants were sensitive to  $\text{Mn}^{2+}$  activation for both fibrinogen and PAC-1 binding, consistent with the  $\alpha 2\beta 1$  and  $\alpha 5\beta 1$  ADMIDAS mutants (22,26). In addition, similar to  $\alpha 2\beta 1$  and  $\alpha 5\beta 1$  integrins, the  $\beta 3$  ADMIDAS mutants bound PAC-1 and fibrinogen with lower affinity than the WT and remained in the bent conformation. Conversely, while remaining in the bent conformation, the ADMIDAS mutants of  $\alpha 4\beta 7$  and  $\alpha L\beta 2$  showed ligand binding at higher levels than the WT (14-15,25). These studies altogether suggest a significant difference in the allosteric properties of the ADMIDAS, and the degree of regulation by the ADMIDAS seems to vary among integrin families.

In the structure of the unliganded low affinity state of the integrin  $\alpha \text{IIb}\beta 3$  (Fig. 1B) (19), the ADMIDAS metal ion coordinates with the main chain carbonyl  $\text{Met}^{335}$  in  $\beta 3$  I domain. This interaction helps to stabilize integrin headpiece in the closed conformation. During inside-out activation, the hybrid domain swings out, leading to the  $\beta$  I domain  $\alpha 7$  helix downward displacement, thus breaking the interaction of the  $\text{Met}^{335}$  and ADMIDAS ion. In this high affinity state with the open headpiece (3), the side chain carboxyl of the  $\text{Asp}^{251}$  moves toward the ADMIDAS site, resulting in direct coordination with the ADMIDAS ion. This shift makes the MIDAS become more positive, resulting in higher affinity for ligands (Fig. 1C) (19). Therefore, the role of ADMIDAS ion in regulating integrin ligand binding is complicated. We propose that

the ADMIDAS ion stabilizes the low affinity state when the integrin headpiece is in the closed conformation, whereas it stabilizes the high affinity state when the headpiece is in the open conformation with the swung-out hybrid domain. In the cases of  $\beta 1$  and  $\beta 3$  integrins, mutating the ADMIDAS residues leads to destabilizing both the high and low affinity states. Therefore, the ADMIDAS mutants reduced, but not abolished ligand binding as shown here and previously (22,26).

But when one ADMIDAS residue of the  $\alpha 4\beta 7$  and  $\alpha L\beta 2$  integrins was mutated, integrins were activated, leading to firm adhesion. It is interesting that in physiological conditions, both  $\alpha 4\beta 7$  and  $\alpha L\beta 2$  integrins mediate cell rolling and firm adhesion, whereas  $\alpha 2\beta 1$ ,  $\alpha 5\beta 1$ , and  $\alpha I\text{Ib}\beta 3$  integrins only mediate firm adhesion (42). When we studied the residues that are potentially important for regulatory effects on ligand binding, we found that one specific amino acid may contribute to these differences (Fig. 1A). The residue after  $\beta 3$  Asp<sup>251</sup> is Ala (and the same for  $\beta 1$  integrins), but the corresponding position in  $\beta 2$  and  $\beta 7$  integrins is Asp. In the open conformation of the  $\alpha I\text{Ib}\beta 3$  crystal structures (3,19), Ala<sup>252</sup> moves approximately 0.7 Å toward the ADMIDAS site along with the Asp<sup>251</sup>. This Ala residue in  $\beta 1$  and  $\beta 3$  may have no effect on ligand binding affinity. Comparing the  $\alpha X\beta 2$  crystal structure with the open and closed  $\alpha I\text{Ib}\beta 3$ , the  $\beta 2$  residue Asp<sup>243</sup>, which corresponds to the  $\beta 3$  residue Ala<sup>252</sup>, points toward the MIDAS ion, and therefore it is expected that this residue decreases ligand binding by increasing the negativity of the MIDAS site (Fig. 1B-D) (17). It has been shown that integrins in the extended conformation with low to intermediate affinity mediate cell rolling, whereas those with high affinity mediate firm adhesion (43). It is likely that the presence of this additional Asp residue in  $\beta 2$  and  $\beta 7$  integrins makes these two families lower affinity for ligands, capable of mediating cell rolling. It is possible that when one ADMIDAS residue Asp is mutated, the binding of ADMIDAS ion was



not abolished; but instead, residues Asp<sup>242</sup> and Asp<sup>243</sup> shift toward the ADMIDAS and both coordinate with the metal ion, leading to a more positive MIDAS able to bind ligands with a higher affinity than the WT. This may explain that mutating ADMIDAS  $\alpha$ L $\beta$ 2 and  $\alpha$ 4 $\beta$ 7 leads to high affinity for ligands, resulting in firm adhesion (14-15,25), contrary to the previous  $\alpha$ 5 $\beta$ 1 and  $\alpha$ 2 $\beta$ 1 studies (22,26) and the present  $\alpha$ IIb $\beta$ 3 work. Additional evidence is needed to confirm this hypothesis.

Our study also showed that by eliminating the ADMIDAS function, integrin outside-in signaling from the ligand binding site to the lower leg in  $\beta$ 3 integrins was abolished. Therefore, even though the ADMIDAS mutants were able to adhere to immobilized ligand, they did not exhibit cell spreading. It has been shown in  $\alpha$ L $\beta$ 2 that the ADMIDAS binds to ICAM-1 but does not trigger the cytoplasmic tail separation and outside-in signaling (25). Therefore, it seems that the ADMIDAS in all integrin families provides a key structural link between the binding site in the  $\beta$  I domain and the hybrid domain for outside-in signaling. It is likely that in order for integrins to transmit signals from the ligand binding site to the lower portion of the molecules, the  $\beta$  I domain must be stabilized in the open conformation in which the ADMIDAS plays a significant role.

## REFERENCES

1. Hynes, R. O. (2002) *Cell* **110**, 673-687
2. Luo, B.-H., Carman, C. V., and Springer, T. A. (2007) *Annu. Rev. Imm.* **25**, 619-647
3. Xiao, T., Takagi, J., Wang, J.-h., Collier, B. S., and Springer, T. A. (2004) *Nature* **432**, 59-67
4. Xiong, J. P., Stehle, T., Zhang, R., Joachimiak, A., Frech, M., Goodman, S. L., and Arnaout, M. A. (2002) *Science* **296**, 151-155
5. Shimaoka, M., Takagi, J., and Springer, T. A. (2002) *Annu. Rev. Biophys. Biomol. Struct.* **31**, 485-516
6. Takagi, J., and Springer, T. A. (2002) *Immunological Rev.* **186**, 141-163
7. Takagi, J., Strokovich, K., Springer, T. A., and Walz, T. (2003) *EMBO J.* **22**, 4607-4615
8. Giancotti, F. G., and Ruoslahti, E. (1999) *Science* **285**, 1028-1032
9. Clark, E. A., and Brugge, J. S. (1995) *Science* **268**, 233-239

10. Kim, M., Carman, C. V., and Springer, T. A. (2003) *Science* **301**, 1720-1725
11. Zhu, J., Carman, C. V., Kim, M., Shimaoka, M., Springer, T. A., and Luo, B.-H. (2007) *Blood* **110**, 2475-2483
12. Mould, A. P., Akiyama, S. K., and Humphries, M. J. (1995) *J. Biol. Chem.* **270**, 26270-26277
13. Burrows, L., Clark, K., Mould, A. P., and Humphries, M. J. (1999) *Biochem. J.* **344 Pt 2**, 527-533
14. Chen, J. F., Salas, A., and Springer, T. A. (2003) *Nat. Struct. Biol.* **10**, 995-1001
15. Chen, J. F., Takagi, J., Xie, C., Xiao, T., Luo, B.-H., and Springer, T. A. (2004) *J. Biol. Chem.* **279**, 55556-55561
16. Mould, A. P., Symonds, E. J., Buckley, P. A., Grossmann, J. G., McEwan, P. A., Barton, S. J., Askari, J. A., Craig, S. E., Bella, J., and Humphries, M. J. (2003) *J. Biol. Chem.* **278**, 39993-39999
17. Xie, C., Zhu, J., Chen, X., Mi, L., Nishida, N., and Springer, T. A. (2010) *EMBO J.* **29**, 666-679
18. Xiong, J.-P., Stehle, T., Diefenbach, B., Zhang, R., Dunker, R., Scott, D. L., Joachimiak, A., Goodman, S. L., and Arnaout, M. A. (2001) *Science* **294**, 339-345
19. Zhu, J., Luo, B. H., Xiao, T., Zhang, C., Nishida, N., and Springer, T. A. (2008) *Molecular Cell* **32**, 849-861
20. Shimaoka, M., Xiao, T., Liu, J.-H., Yang, Y., Dong, Y., Jun, C.-D., McCormack, A., Zhang, R., Joachimiak, A., Takagi, J., Wang, J.-h., and Springer, T. A. (2003) *Cell* **112**, 99-111
21. Lee, J.-O., Rieu, P., Arnaout, M. A., and Liddington, R. (1995) *Cell* **80**, 631-638
22. Mould, A. P., Barton, S. J., Askari, J. A., Craig, S. E., and Humphries, M. J. (2003) *J. Biol. Chem.* **278**, 51622-51629
23. Whittaker, C. A., and Hynes, R. O. (2002) *Mol. Biol. Cell* **13**, 3369-3387
24. Hynes, R. O., and Zhao, Q. (2000) *J. Cell. Biol.* **150**, F89-F96
25. Chen, J. F., Yang, W., Kim, M., Carman, C. V., and Springer, T. A. (2006) *Proc. Natl. Acad. Sci. U S A* **103**, 13062-13067
26. Valdramidou, D., Humphries, M. J., and Mould, A. P. (2008) *The Journal of Biological Chemistry* **283**, 32704-32714
27. Gotwals, P. J., Chi-Rosso, G., Ryan, S. T., Sizing, I., Zafari, M., Benjamin, C., Singh, J., Venyaminov, S. Y., Pepinsky, R. B., and Kotliansky, V. (1999) *Biochemistry* **38**, 8280-8288
28. Harding, M. M. (2001) *Acta Crystallogr. D Biol. Crystallogr.* **57**, 401-411
29. Murcia, M., Jirouskova, M., Jihong, L., Coller, B. S., and Filizola, M. (2008) *Proteins* **71**, 1779-1791
30. Salas, A., Shimaoka, M., Kogan, A. N., Harwood, C., von Andrian, U. H., and Springer, T. A. (2004) *Immunity* **20**, 393-406
31. Kamata, T., Tieu, K. K., Tarui, T., Puzon-McLaughlin, W., Hogg, N., and Takada, Y. (2002) *J. Immunol.* **168**, 2296-2301
32. Luo, B.-H., Takagi, J., and Springer, T. A. (2004) *J. Biol. Chem.* **279**, 10215-10221
33. Bajt, M. L., and Loftus, J. C. (1994) *J. Biol. Chem.* **269**, 20913-20919
34. Takagi, J., Petre, B. M., Walz, T., and Springer, T. A. (2002) *Cell* **110**, 599-611
35. Luo, B.-H., Springer, T. A., and Takagi, J. (2003) *Proc. Natl. Acad. Sci. U. S. A.* **100**, 2403-2408

36. Wang, W., Fu, G., and Luo, B.-H. (2010) *Biochemistry*
37. Beglova, N., Blacklow, S. C., Takagi, J., and Springer, T. A. (2002) *Nat. Struct. Biol.* **9**, 282-287
38. Du, X., Gu, M., Weisel, J. W., Nagaswami, C., Bennett, J. S., Bowditch, R., and Ginsberg, M. H. (1993) *J. Biol. Chem.* **268**, 23087-23092
39. Tozer, E. C., Liddington, R. C., Sutcliffe, M. J., Smeeton, A. H., and Loftus, J. C. (1996) *J. Biol. Chem.* **271**, 21978-21984
40. Yamanouchi, J., Hato, T., Tamura, T., and Fujita, S. (2002) *Thromb. Haemost.* **87**, 756-762
41. Baker, E. K., Tozer, E. C., Pfaff, M., Shattil, S. J., Loftus, J. C., and Ginsberg, M. H. (1997) *Proc. Natl. Acad. Sci. U.S.A.* **94**, 1973-1978
42. McEver, R., and Zhu, C. (2010) *Annual Review of Cell and Developmental Biology* **26**, 363-396
43. Salas, A., Shimaoka, M., Phan, U., Kim, M., and Springer, T. A. (2006) *J. Biol. Chem.* **281**, 10876-10882

### FOOTNOTES

We thank the American Heart Association (#10GRNT3960011) and the Louisiana Board of Regents (LEQSF(2009-12)-RD-A07) for financial support.

## FIGURES

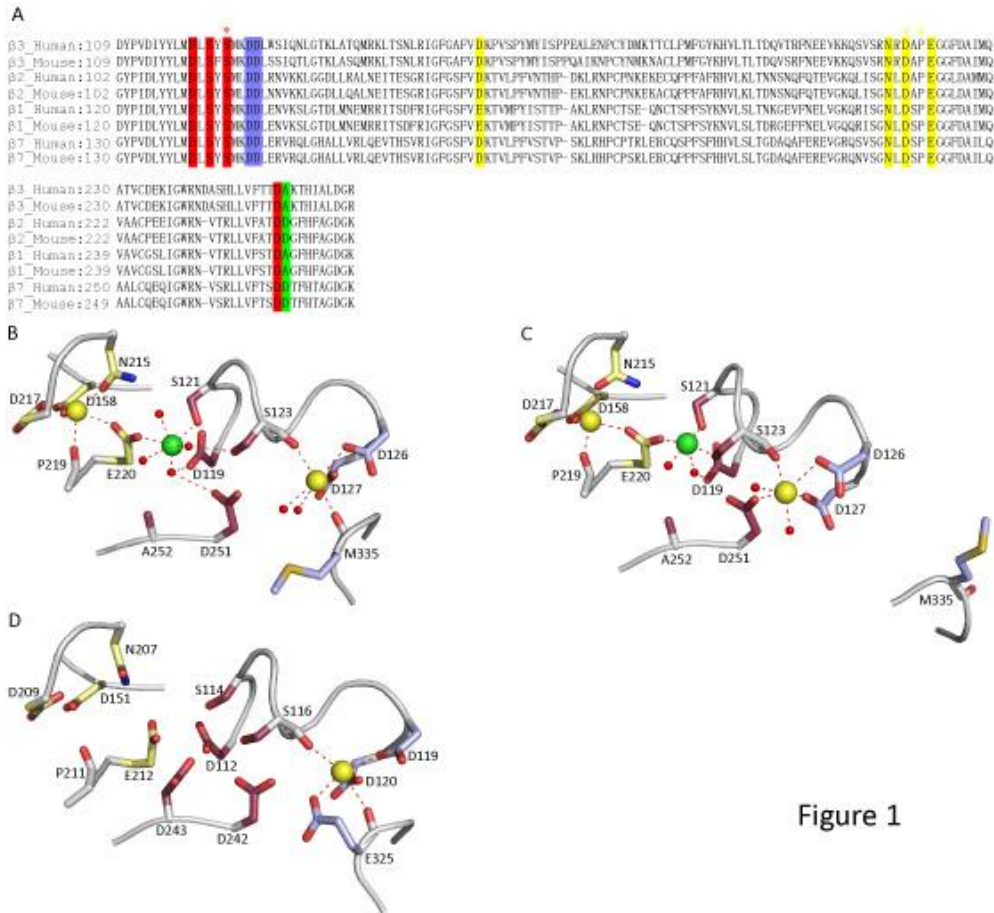
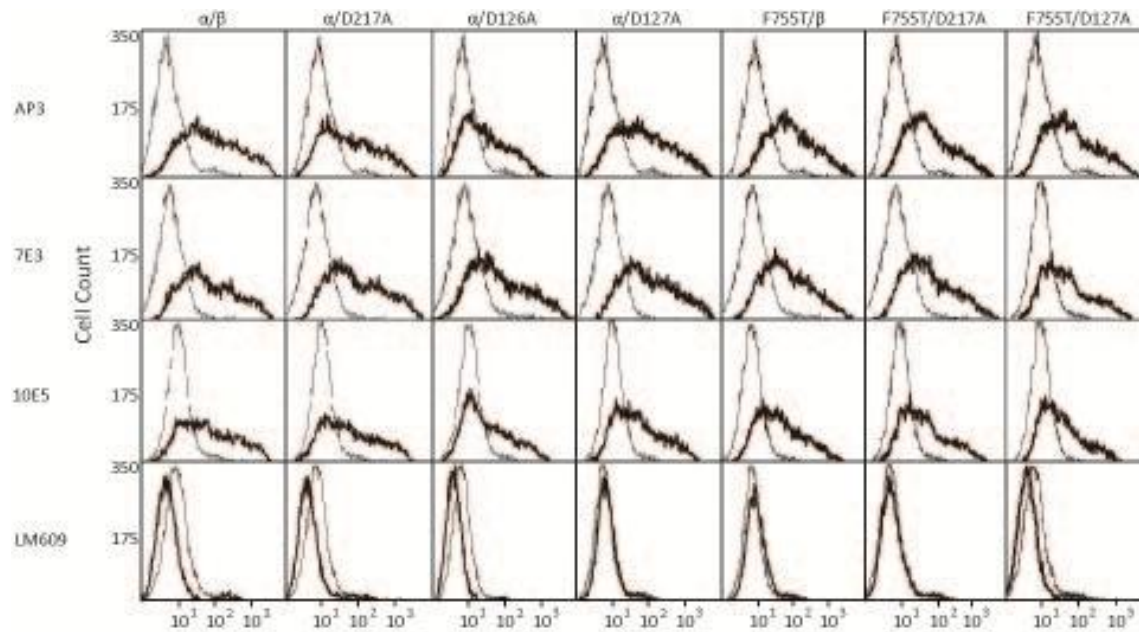


Figure 1

**Figure 1.  $\beta$  subunit Sequence Alignment and Structure of Metal-Binding Sites in  $\alpha$ IIb $\beta$ 3 and  $\alpha$ X $\beta$ 2.** (A) Sequence alignment of human  $\beta$ 1,  $\beta$ 2,  $\beta$ 3, and  $\beta$ 7 I domain metal ion binding sites. Residues with metal-coordinating side-chain oxygen atoms are highlighted, and residues with metal-coordinating backbone carbonyl oxygen atoms are asterisked. Highlighted or asterisked residues are colored as MIDAS, red; SyMBS, yellow; and ADMIDAS, light blue. Structure of unliganded (B) and liganded (C)  $\alpha$ IIb $\beta$ 3 metal-binding sites. (D) Structure of unliganded  $\alpha$ X $\beta$ 2 metal-binding sites. The metal-binding sites are colored as follows: raspberry, MIDAS; pale yellow, SyMBS; light blue, ADMIDAS. N and O atoms involved in metal coordinating side chains or carbonyl backbones are colored in blue and red, respectively.  $\text{Ca}^{2+}$  and  $\text{Mg}^{2+}$  ions are colored in yellow and green, respectively. Polar coordination between O atoms and metal ions are shown by dashed red lines.



**Figure 2**

**Figure 2. Expression of WT and Mutant  $\alpha$ IIb $\beta$ 3 Integrins.** Using immunofluorescent flow cytometry, HEK293T transfectants were labeled with AP3 (anti- $\beta$ 3), 7E3 (anti- $\beta$ 3), 10E5 (anti- $\alpha$ IIb), and LM609 (anti- $\alpha$ V). Thick and thin lines show labeling of the  $\alpha$ IIb $\beta$ 3 transfectant and the mock transfectant, respectively.

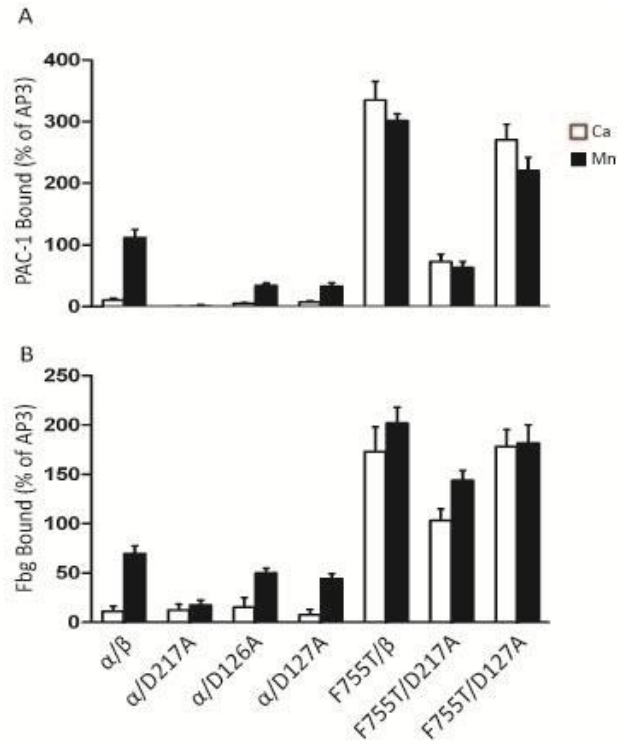


Figure 3

**Figure 3. Soluble Ligand Binding with PAC-1 and Fibrinogen.** Cells were incubated with (A) PAC-1 in the presence of 5 mM  $\text{Ca}^{2+}$  or 1 mM  $\text{Mn}^{2+}$ , or (B) FITC-fibrinogen in the presence of 5 mM  $\text{Ca}^{2+}$  or 1 mM  $\text{Mn}^{2+}$  as indicated. Binding activities were determined by flow cytometry and expressed as described in Materials and Methods. Error bars are standard deviation (SD).

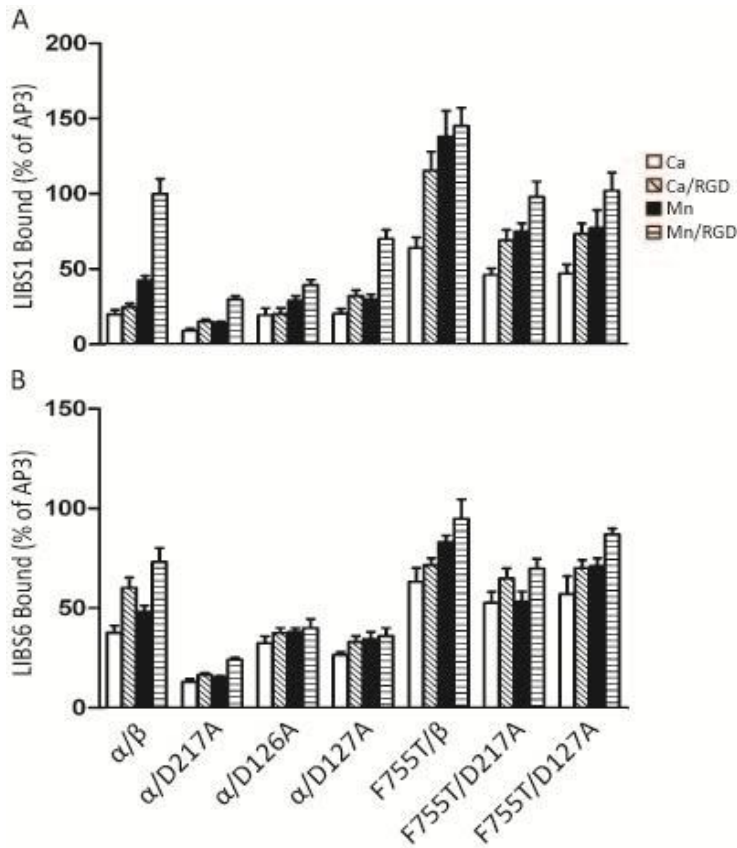


Figure 4

**Figure 4. Exposure of the LIBS1 and LIBS6 epitope.** Cells were stained with (A) anti-LIBS antibody LIBS1 and (B) anti-LIBS antibody LIBS6 in the presence of 5 mM  $\text{Ca}^{2+}$ , 5 mM  $\text{Ca}^{2+}$  plus 50  $\mu\text{M}$  RGD peptides (GRGDSP), 5 mM  $\text{Mn}^{2+}$ , or 5 mM  $\text{Mn}^{2+}$  plus 50  $\mu\text{M}$  RGD peptides. LIBS epitope exposure was determined as the percentage of MFI of anti-LIBS1 antibody relative to non-functional anti- $\beta 3$  mAb AP3. Error bars are SD.

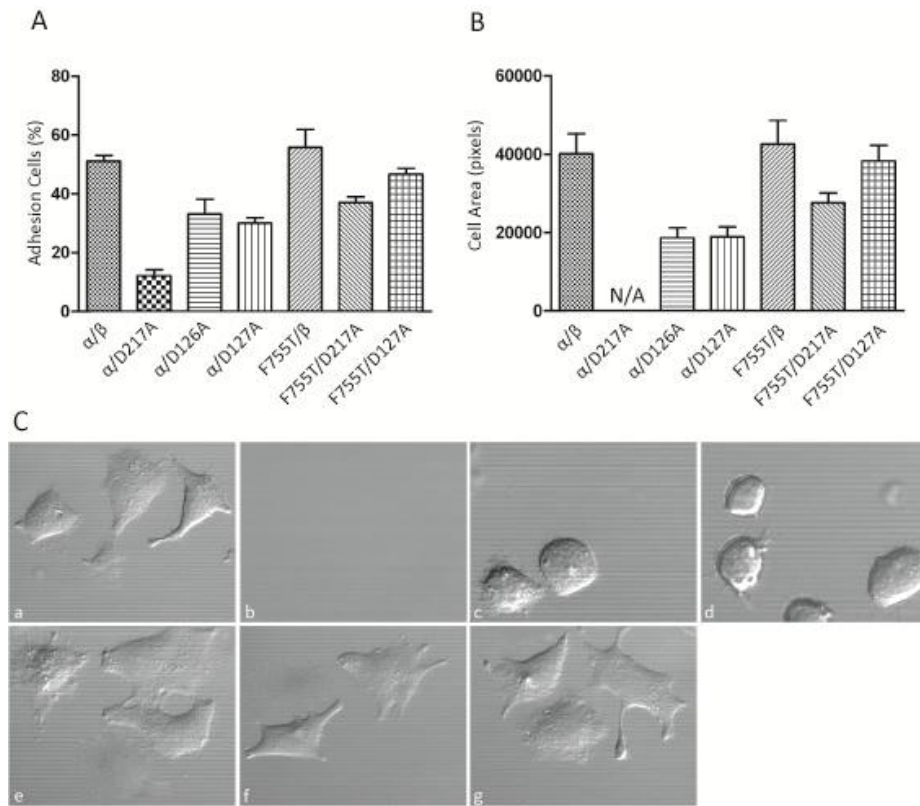


Figure 5

**Figure 5. Cell adhesion and spreading.** A. Adhesion of HEK293T transfectants to surfaces coated with 20  $\mu\text{g/ml}$  fibrinogen. The amount of bound cells was determined by measuring LDH activity as described in Materials and Methods. Data are representative of three independent experiments, each in triplicate. B. Quantification of the areas of adhering/spreading cells as described in Materials and Methods. Error bars are SD. C. DIC images of HEK293T transfectants after adhering to immobilized fibrinogen at 37 °C. a: WT; b: D217A; c: D126A; d: D127A; e: F755T/WT; f: F755T/D217A; g: F755T/D127A. The images are representatives of three independent experiments.